https://doi.org/10.5194/egusphere-2025-3030
Preprint. Discussion started: 7 August 2025

Quantifying the interplay of Meltwater and Ice-Albedo Feedbacks in the Arctic Ice-Ocean System

Haohao Zhang[1, 2, 3], Andrea Storto[2], Xuezhi Bai[1, 3] and Chunxue Yang[2]

[1]College of Oceanography, Hohai University, Nanjing 210024, China.
[2]Institute of Marine Sciences (ISMAR), National Research Council (CNR), Rome, Italy.
[3]Key Laboratory of Marine Hazards Forecasting, Ministry of Natural Resources, Hohai University, Nanjing 210024, China.

Correspondence to: Xuezhi Bai (xuezhi.bai@hhu.edu.cn)

Abstract. Sea ice melting generates multiple feedbacks through meltwater release and open water expansion. Due to the tight coupling of the ice-ocean system, these feedbacks are challenging to quantify independently. We employ a well-validated one-dimensional coupled sea ice-ocean model, by removing meltwater or keeping sea ice constant during the melting season, to quantify the independent effects of meltwater and ice-albedo feedbacks on the Arctic ice-ocean system. The experiments reveal the following: (1) Meltwater-induced strong stratification can insulate a portion of solar radiation into the Near Surface Temperature Maximum (NSTM), generating a negative feedback with a feedback factor of -0.19 (i.e., 19% ice melting reduction). (2) The ice-albedo positive feedback factor is +0.41 (i.e., 41% ice melting amplification). (3) These two feedback processes exhibit nonlinear interdependence: switching off the ice-albedo feedback reduces the meltwater feedback strength to -0.09, while eliminating meltwater effects enhances the ice-albedo feedback to +0.46. Meltwater effects persist until the following freezing season. The NSTM insulated by meltwater in summer suppresses ice formation during winter in strongly stratified regions. In the weakly stratified western Nansen Basin, summer meltwater release plays an important role in preventing the upward mixing of Atlantic warm water. The meltwater feedback in the ice-ocean system is more pronounced in experiments with thinner initial sea ice, indicating that as Arctic sea ice will continue to decline and Atlantification will intensify in the future, the impact of meltwater on the ice-ocean system is expected to become increasingly significant.

https://doi.org/10.5194/egusphere-2025-3030
Preprint. Discussion started: 7 August 2025

1 Introduction

The vertical structure of the Arctic Ocean is characterized by a cold and fresh surface mixed layer (ML) overlying a cold halocline layer (CHL) and the Atlantic warm water (AWW) layer at depth. The fresh surface ML is largely influenced by the seasonal cycle of sea ice melting and freezing (Hordoir et al., 2022; Morison and Smith, 1981; Peralta-Ferriz and Woodgate, 2015; Polyakov et al., 2013), while the CHL originates from waters formed on shallow shelves and in the Arctic proper during ice formation, along with the resultant brine rejection (Alkire et al., 2017; Rudels et al., 2004). The CHL effectively reduces heat flux to the surface ML from the AWW below due to its coincidence of near-freezing temperatures and strong salinity gradient (Aagaard et al., 1981; Rudels et al., 1996; Steele and Boyd, 1998). In summary, the sea ice melt-freeze cycle is a key process in regulating ocean stratification and AWW layer ventilation through meltwater input and brine rejection.

Over the past few decades, the extent of Arctic sea ice has shown significant negative trends characterized by a regime shift from multi-year ice to seasonal ice dominance (Kwok, 2018; Moon et al., 2021; Mioduszewski et al., 2019; Serreze and Meier, 2019; Sumata et al., 2023), indicating that the seasonal melt-freeze cycle is intensifying. The freshwater input from external sources plays an important role in the long-term freshwater balance and stratification changes in the Arctic Ocean (Carmack et al., 2016; Forryan et al., 2019; Nummelin et al., 2016; Serreze et al., 2006). On seasonal scales, the release of meltwater is the dominant factor influencing stratification changes (Hordoir et al., 2022; Peralta-Ferriz and Woodgate, 2015). During the melting season, approximately 11,300 km^3 of meltwater is discharged into the Arctic Ocean, which is an order of magnitude greater than the annual net freshwater input from external sources (1,200 km^3), which includes river runoff (4,200 km^3), precipitation minus evaporation (P-E, 2,200 km^3), and the net fluxes through oceanic gateways (-5,200 km^3) (Haine et al., 2015). Notably, on seasonal scales, runoff tends to remain confined to the coastal regions of the Arctic Ocean (Osadchiev et al., 2017, 2021), with its transport pathways influenced by atmospheric circulation regimes (Wang et al., 2021). The meltwater volume of 11,300 km³ divided by the area of the Arctic Ocean (about 9.7×10^6 km^2, excluding the Canadian Arctic Archipelago and Baffin Bay) equivalent to an average of 1.2 m of freshwater temporarily being deposited into the Arctic Ocean surface each summer (Haine et al., 2015), freshening and stabilizing the upper ocean. It isolates a portion of the solar radiation heat entering the ocean into the base of the mixed layer, thereby forming the Near-Surface Temperature Maximum (NSTM) (Hudson et al., 2013; Jackson et al., 2010), which helps to slow down the ice melting during summer (Perovich et al., 2021; Zhang et al., 2023). In winter, brine rejection caused by ice formation leads to the upward entrainment of heat from the NSTM and AWW and impedes winter ice formation consequently (Smith et al., 2018; Steele et al., 2011; Timmermans et al., 2017), which is a negative feedback known as the ice production-entrainment feedback (Goosse et al., 2018).

Sea ice melting not only influences the ice-ocean system by altering ocean surface freshwater fluxes (SFW), but also leads to the expansion of open-water areas, which also generates significant feedback effects on ocean stratification and the ice itself by altering ocean vertical heat transport (Fine et al., 2023; Polyakov et al., 2017; Polyakov et al., 2020; Landrum et al., 2022). On the one hand, the reduction in sea ice cover facilitates increased momentum transfer from the atmosphere to the Arctic Ocean, resulting in enhanced vertical mixing (Armitage et al., 2020; Krishfield et al., 2014; Martin et al., 2016; Wang

https://doi.org/10.5194/egusphere-2025-3030
Preprint. Discussion started: 7 August 2025

et al., 2024). On the other hand, it allows greater penetration of solar radiation into the ocean, contributing to further melting of sea ice (Himmich et al., 2024; Holland et al., 2006; Jenkins and Dai, 2021; Thackeray and Hall, 2019; Uhlíková et al., 2025; Winton, 2006). Consequently, any change in the melt-freeze cycle and the strength of stratification can have significant impacts on each other, through a complex series of feedback processes in the ice-ocean system.

Under the current climate conditions of rapid Arctic warming and intensifying sea ice melt-freeze cycles, separate quantification of the feedbacks induced by meltwater release and ice loss is crucial for understanding the coupling mechanisms and the relative importance of the various components of the Arctic ice-ocean system, as well as for predicting future climate change. Due to the nearly inseparable coupling within the ice-ocean system and many feedbacks are strongly non-linear, conducting an isolated quantitative study of the feedback mechanisms involved in the ice melting process is challenging. Indeed, there are only a few studies that specifically quantify the impact of meltwater in the Arctic ice-ocean system. Zhang et al., (2023) demonstrated that the removal of meltwater increases ice melt by 17%. However, this value was obtained under the condition of initial sea ice thickness of 2.5 m, whereas the current Arctic Ocean actually has thinner ice thickness across most regions (Kacimi and Kwok, 2022; Kwok et al., 2020; Landy et al., 2022). Additionally, it is largely unknown how important is the meltwater feedback compared to the ice-albedo feedback that currently has a profound impact on the Arctic Ocean. To complicate the question, the regional differences in the vertical structure of the Arctic Ocean - characterized by a gradual weakening of stratification strength from the Amerasian Basin to the Eurasian Basin (Polyakov et al., 2013; Toole et al., 2010) - lead to spatially varying impact of meltwater on ice-ocean system. Based on the above, the specific issues that this study primarily focuses on are:

(1) To what extent do the meltwater and ice-albedo feedbacks influence ice melting during summer?

(2) What is the contribution of the meltwater (ice-albedo) feedback if the ice-albedo (meltwater) feedback is not involved?

(3) What are the regional differences in the impact of meltwater on the ice-ocean system?

To study these three questions, we used an idealized one-dimensional (1D) coupled sea ice-ocean model, employing the methods of either removing the meltwater flux at the ocean surface or maintaining a constant ice cover during the melting season, fully or partially decoupling the interactions between sea ice and the ocean in the model, thereby preventing the independent effects of the meltwater feedback and ice-albedo feedback. For various feedbacks in polar regions, Goosse et al. (2018) proposed a simple and consistent method to quantify these feedbacks, and we combine this approach with our model experiments to quantify these two feedbacks. 1D models have been widely used in previous studies of the Arctic Ocean's vertical structure and ice cover (Björk et al., 2002; Davis et al., 2016; Nummelin et al., 2015; Wang et al., 2024; Linders and Björk, 2013; Toole et al., 2010; Zhang et al., 2023). When advection flux effects are not considered, 1D model is a simple and effective tool that can simulate a reasonable upper ocean stratification in short-term simulations. To the best of our knowledge, this is the first study to quantify the above feedback effects based on a coupled ice-ocean model, both individually and in combination, while also examining the varying initial stratifications across different Arctic regions, to assess their relative impacts throughout the annual cycle.

https://doi.org/10.5194/egusphere-2025-3030
Preprint. Discussion started: 7 August 2025

The structure of this paper is as follows: Section 2 details the 1D model and experimental design. Section 3 presents the model results. Section 4 calculates the feedback factors. Section 5 discusses the results. Section 6 summarizes the main achievements. In the Supporting Information (SI), we provide additional text and figures detailing the validation and performance of the coupled sea ice-ocean model.

2 Materials and Methods

2.1 One-dimensional model

The model used in this study is a 1D coupled sea ice-ocean model based on the Massachusetts Institute of Technology General Circulation Model (MITgcm, Marshall et al., 1997). The ocean model utilizes the nonlinear equation of state of Jackett and Mcdougall, (1995) and the vertical mixing is parameterized by the nonlocal K-Profile Parameterization (KPP) scheme of Large et al., (1994). The background vertical diffusivity in this model is set to $5.44 \times 10^{-7}\ m^2 s^{-1}$, following Nguyen et al., (2011) in their Arctic regional model based on MITgcm. Several observation-based studies have shown that the vertical diffusivity in the deep central Canadian Basin averages near-molecular levels between $2.2 \times 10^{-7}\ m^2 s^{-1}$and $3.4 \times 10^{-7}\ m^2 s^{-1}$ (Shaw and Stanton, 2014) and it averages $10^{-6}\ m^2 s^{-1}$ in the deep interior basins (Fer, 2009; Rainville and Winsor, 2008). Therefore, the choice of background vertical diffusivity is not uniform in various models, ranging from $10^{-7}\ m^2 s^{-1}$ to $10^{-6}\ m^2 s^{-1}$ (Liang and Losch, 2018; Linders and Björk, 2013; Nummelin et al., 2015; Toole et al., 2010). To check the uncertainty in our experimental results due to the choice of background mixing coefficients, we conducted experiments using the three coefficients of $10^{-7}\ m^2 s^{-1}$, $5.44 \times 10^{-7}\ m^2 s^{-1}$ and $10^{-6}\ m^2 s^{-1}$ and compared their differences. The results showed that selecting any of these three mixing coefficients did not significantly affect our experimental results. The differences between the experimental results using different mixing coefficients are detailed in Figures S1-S4 in the SI.

The water column in the model extends from the surface down to a depth of 700 m, with the vertical grid maintaining a uniform thickness of 1 m. No boundary condition is applied at the bottom of the model. We also verified that adding a sponge layer with a 1-day recovery period in the bottom 100 m results in no significant difference in the results compared to the case without any bottom boundary conditions (Figures S5-S8 in SI), because the depth of the model is deep enough. The sea ice model is based on a variant of the viscous-plastic sea ice model (Losch et al., 2010) and combined with a thermodynamic ice model, which is based on the 3-layer model by Winton (2000) and the energy-conserving LANL CICE model (Bitz and Lipscomb, 1999). A more detailed description of the sea ice model can be found in Appendix A.

The model simulated a period of one year, from May 1 to next April 30, intending to conduct a full melting period followed by a complete freezing phase in the model, which helps to better investigate the effects of meltwater on sea ice melting in summer, as well as its impact on subsequent freezing in winter. Linders and Björk (2013) used a similar method in their study, but in order to experience a freezing season followed by a thawing season, their experiment was conducted from September to the next August.

https://doi.org/10.5194/egusphere-2025-3030
Preprint. Discussion started: 7 August 2025

2.2 Initial conditions

For the ocean initial conditions, the initial profiles of temperature and salinity used in the model runs (Figure 1) are conductivity-temperature-depth (CTD) profiles taken from the World Ocean Database 2023 (WOD23, Mishonov et al., 2024) and Ice-Tethered Profiles (ITP, Krishfield et al., 2008; Toole et al., 2011, 2016). We selected 20 profiles as the initial profiles for the 1D model, distributed in different basins of the Arctic Ocean (Figure 1). The chosen profiles are from the late of the freezing season, February to May, between 2011-2023 (color scale in Figure 2), in order to match the beginning of the model simulations, close to the beginning of the melting season. The buoyancy frequencies of these profiles indicate a gradual decrease in the strength of ocean stratification from the Pacific side towards the Atlantic side (Figure 2, where, in order to emphasize the regional differences of the upper stratification, we show only the upper 300 m). These 20 profiles represent diverse stratification characteristics across the whole Arctic Basin.

For the initial conditions of sea ice model, based on satellite observations, between 2011 and 2020, the basin-averaged Arctic sea ice thickness is 1.87 ± 0.10 m (mean ± standard deviation) at the start of the melting season in May (Landy et al., 2022). Therefore, each set of experiments includes two different initial sea ice thickness (SIT) conditions, 1.5 m and 2 m, to represent the possibly different melting cycles within thin (seasonal) or thick (multi-annual) sea ice scenarios. The initial sea ice concentration (SIC) is about 96%, climatological Arctic basin-averaged, north of the Bering Strait and the Fram Strait and Excluding the Canadian Archipelago, for May 2011-2023 calculated from the sea ice concentration dataset of National Snow and Ice Data Center (NSIDC). The initial snow thickness of the model is set to 0.19 m, based on the basin-averaged Arctic snow thicknesses in April observed by satellite, as reported by Kwok et al., (2020) and Kacimi and Kwok, (2022).

https://doi.org/10.5194/egusphere-2025-3030
Preprint. Discussion started: 7 August 2025

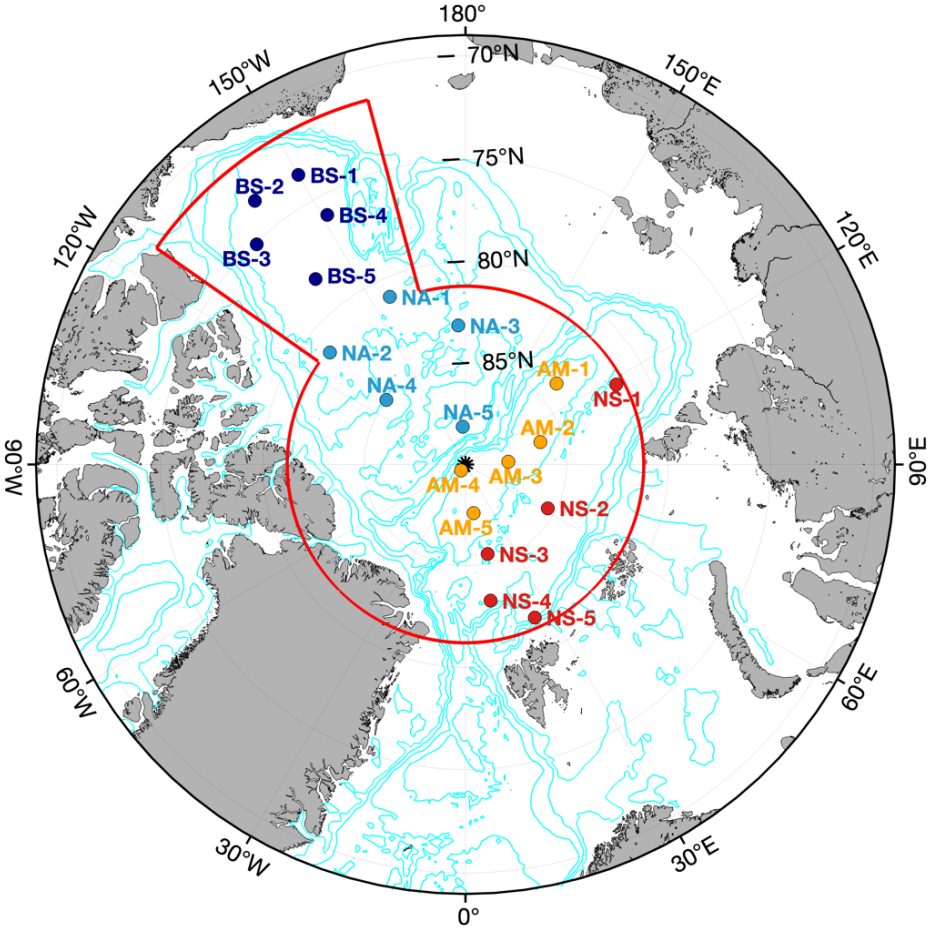

Figure 1. Locations of the observational data used as initial profiles in the model. The same atmospheric forcing field, based on the 2011-2023 climatological daily average for the region defined by the solid red line, is used in all experiments. BS1 to BS5, located in the Beaufort Sea (dark blue dots); NA1 to NA5 located in the North of the Amerasian Basin (cyan dots); AM1 to AM5 located in the Amundsen Basin (the green dots); NS1 to NS5 located in the Nansen Basin (the red dots). BS: Beaufort Sea; NA: North American Basin; AM: Amundsen Basin; NS: Nansen Basin. The thin blue lines represent isobaths of 100, 500, 1000 and 3000 m.

https://doi.org/10.5194/egusphere-2025-3030
Preprint. Discussion started: 7 August 2025

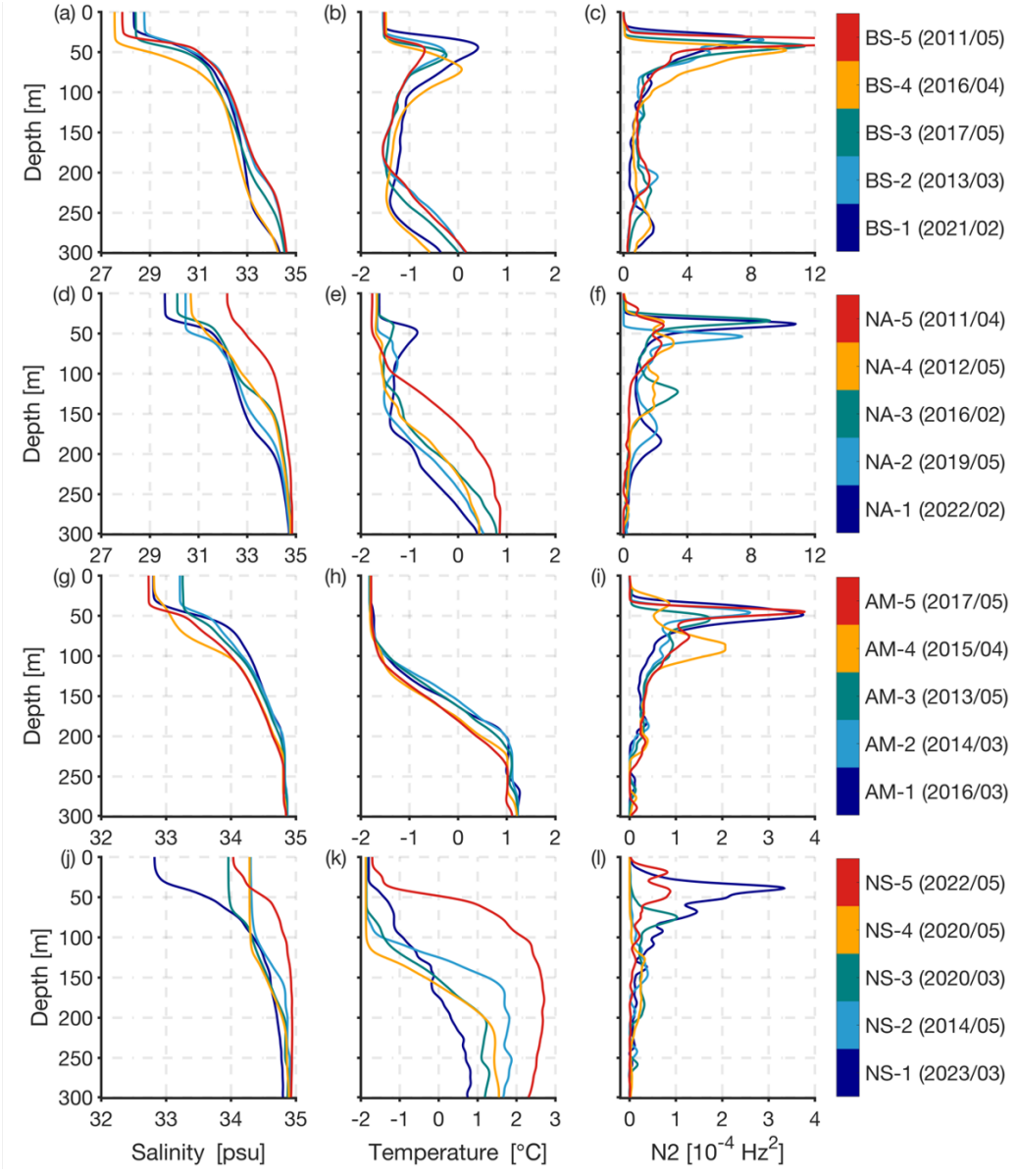

Figure 2. Observed salinity (left column), temperature (middle column) and buoyancy frequency (right column) from observational profiles between 2011 and 2023 in the Arctic Ocean, used as initial profiles in the model simulations. The buoyancy frequency is calculated based on temperature, salinity, and depth. The profiles are arranged after geographical location with the aim to capture the typical characteristics of each region. (a)-(c): Beaufort Sea (BS); (d)-(f): North of the Amerasian Basin (NA); (g)-(i): Amundsen Basin (AM); (j)-(l): Nansen Basin (NS). The time of each profile is shown in the color scale at the right-hand side. In order to emphasize the regional differences of the upper stratification, we show only the upper 300m. In fact, in the model we used the upper 700 m of data as the initial field. Note that for clearer display of the values of the profiles, the x-axis of (a)-(f) are inconsistent with that of (g)-(l).

https://doi.org/10.5194/egusphere-2025-3030
Preprint. Discussion started: 7 August 2025

2.3 Forcing

The atmospheric forcing for the 1D model consists of daily averages of 10 m wind speed, 2 m air temperature, specific humidity, sea level pressure, downward longwave and shortwave radiation, all derived from the National Centres for Environmental Prediction-Department of Energy (NCEP-DOE) Reanalysis 2 (Kanamitsu et al., 2002). The forcing field of the 1D model utilizes regional and climatological daily averages. The period used for the climatology average is from 2011 to 2023 and the regions are derived from two subareas: the Central Arctic Ocean, spanning latitudes 81.2° to 90° N and longitudes 0° to 360° E, and the Canada Basin, spanning latitudes 71.5° to 81.2° N and longitudes 195° to 235° E, as delineated within the red boundary in Figure 1. For external net freshwater flux, Davis et al., (2016) utilized a time- and area-averaged method in their 1D model. Haine et al., (2015) reported that net inflow of freshwater into the Arctic Ocean is approximately 1200 km^3 per year, when it divided by the area of the Arctic ($9.7 \times 10^6\ km^2$), this corresponds to an average input of $3.92 \times 10^{-9}\ m/s$ (based on the 365-day), which is applied at the surface of our model to represent the external freshwater input, and it is verified that it is a reasonable choice in this 1D model (Section 1.3 and Figure S9 in SI).

2.4 Experiments

Based the feedback factor (γ) framework proposed by Goosse et al. (2018), when only one feedback is operating, the feedback factor γ can be quantified as the ratio between the additional changes specifically due to the feedback and the response of the full system including all the feedbacks (Total response, TR). This additional change is itself computed as the difference between the response of the full system and the one of a reference system in which the feedback under consideration does not operate (Reference response, RR), if γ is a positive (negative) value, it represents positive (negative) feedback:

$$\gamma = \frac{TR-RR}{TR} \quad (1)$$

In the coupled sea ice-ocean model, the feedback induced by meltwater discharge during melting season is intricately coupled with ice-albedo feedback driven by ice loss, making their independent roles inseparable through conventional single-variable experiments. To overcome this limitation, we designed four progressively constrained sensitivity experiments (Table 1). We artificially create a system devoid of meltwater feedback by setting the ocean meltwater flux to zero (Figure 3b). In addition, we switch off the ice-albedo feedback by maintaining constant summer sea ice concentration and thickness (Figure 3c). Figure 4 shows details of the time development of the simulation results for station BS5 with initial SIT of 2 m, helping to understand the procedures of the four experiments more clearly, and the detailed analysis of these results present in the Section 3.

(1) CTRL: the baseline experiment, which simulates natural ice melting processes with the full coupled ice-ocean system including all the feedback processes (Figure 3a).

https://doi.org/10.5194/egusphere-2025-3030
Preprint. Discussion started: 7 August 2025

(2) noMW: the meltwater flux is set to zero during the melting season in the model to exclude meltwater feedback, while allowing ice thickness to decrease freely (Figure 3b). Figure 4 illustrates a reduction in sea ice during the summer (Figure 4b and c), while the SFW remains zero (Figure 4d).

(3) noIA: we artificially maintain constant sea ice thickness and concentration during the melting season in the model (i.e., fixed to the value of the first melt-day), while still permitting meltwater discharge (Figures 3c). As shown in Figure 4, summer sea ice thickness and concentration remain unchanged, but SFW is not zero.

In addition, we also want to explore the net ice-albedo feedback and meltwater feedback. Therefore, we designed the following experiment:

(4) noMWIA: based on the noIA configuration but setting meltwater flux to zero (Figure 3d) to eliminate both ice-albedo feedback and meltwater feedback.

There are three points to note: First, in the noIA and noMWIA runs, we artificially kept sea ice constant in the model to limit the ice-albedo feedback, which means we cannot get the actual ice melting thickness from the sea ice diagnostic of the model output. However, we can obtain it as an offline diagnostic using Eq (A5). Second, compared to the meltwater flux, the SFW caused by other processes (e.g., evaporation and external freshwater forcing) is minimal. For example, Figure 4d shows that, after removing the meltwater, the SFW is nearly zero. Third, all imposed constraints are enforced exclusively during the melting season, with the model reverting to natural ice-ocean coupling during freezing season. This design enables explicit assessment of how summer-imposed interventions modulate the winter evolution of the naturally coupled ice-ocean system.

These experiments systematically decouple the effects of meltwater discharge from ice-albedo feedback caused by ice loss through imposing targeted variable constraints, enabling to quantify precisely both the independent meltwater feedback and its relative contribution compared to ice-albedo feedback. Through these four experimental sets, combined with the methodology of Goosse et al., (2018), we quantitatively assess the feedback factors (detailed in Section 4). Although our experimental design is somewhat idealized, this approach can directly illustrate the independent impacts of meltwater on the ice-ocean system and their relative importance. The 1D model used in this study has been demonstrated capable of well simulating the seasonal variations in the vertical temperature-salinity structure, sea ice and ocean-ice heat flux in the Arctic Ocean (Section 1.4 in SI and Zhang et al., 2023).

Table 1. Experiment matrix

Experiment	Sea ice evolution	Meltwater Flux	Purpose
(1) CTRL	Prognostic	Natural	Baseline under natural state
(2) noMW	Prognostic	Zeroed	No meltwater feedback
(3) noIA	Fixed (first melt-day state)	Natural	No ice-albedo feedback
(4) noMWIA	Fixed (first melt-day state)	Zeroed	No ice-albedo and meltwater feedbacks

Note: all imposed constraints are enforced exclusively during the melting season, with the model reverting to natural ice-ocean coupling during freezing season.

https://doi.org/10.5194/egusphere-2025-3030
Preprint. Discussion started: 7 August 2025

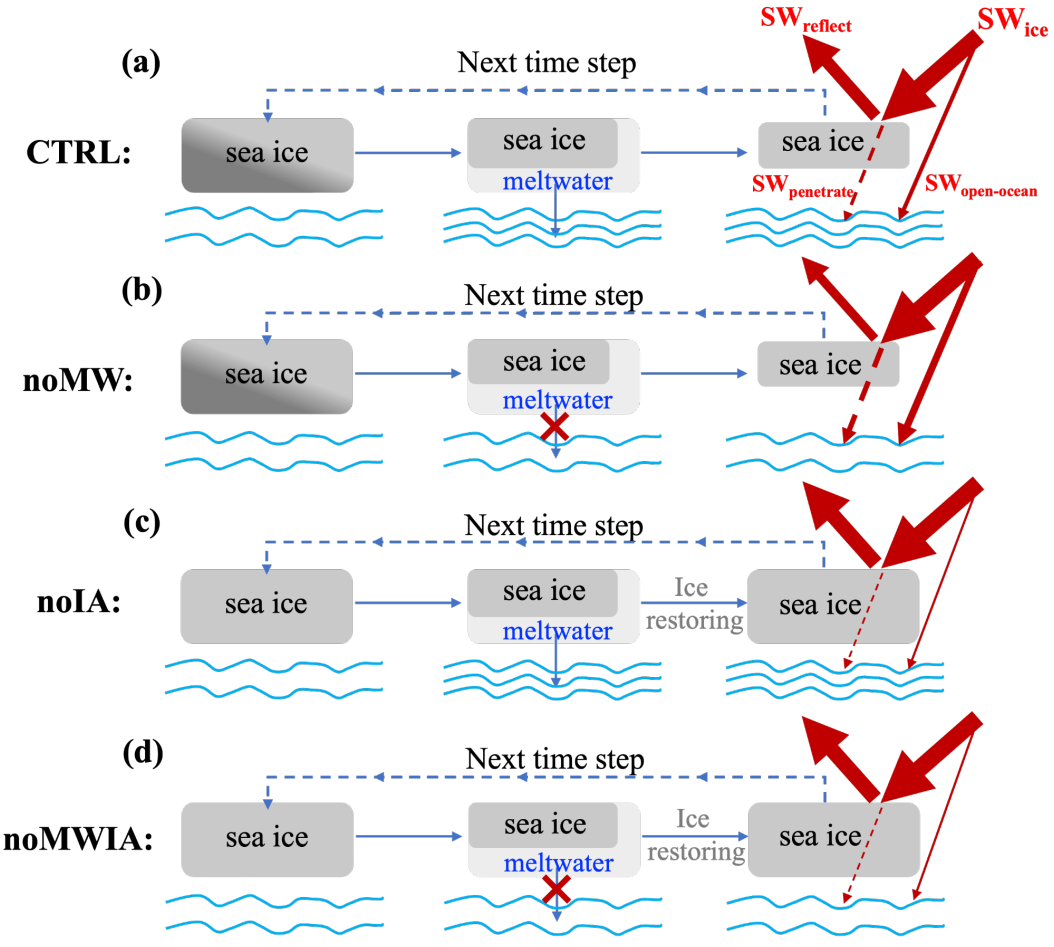

Figure 3. Schematic representation of the four experiments in this study. (a): CTRL, ice-ocean coupled model running normally; (b): noMW, after sea ice melting, the meltwater flux entering the ocean is set to 0; (c): noIA, after sea ice melting, meltwater enters the ocean normally, but before the model starts the next time step, sea ice is restored to its first melt-day state; (d): noMWIA, After sea ice melts, the meltwater flux entering the ocean is set to 0, and simultaneously, before the model starts the next time step, the sea ice is restored to its first melt-day state. The red arrows represent the shortwave radiation fluxes. SWice: Shortwave radiation reaching the ice surface; SWreflect: shortwave radiation reflected from the ice surface; SWpenetrate: shortwave radiation penetrating sea ice and reaching the ocean; SWopen-ocean: shortwave radiation entering the ocean through open ocean.

https://doi.org/10.5194/egusphere-2025-3030
Preprint. Discussion started: 7 August 2025

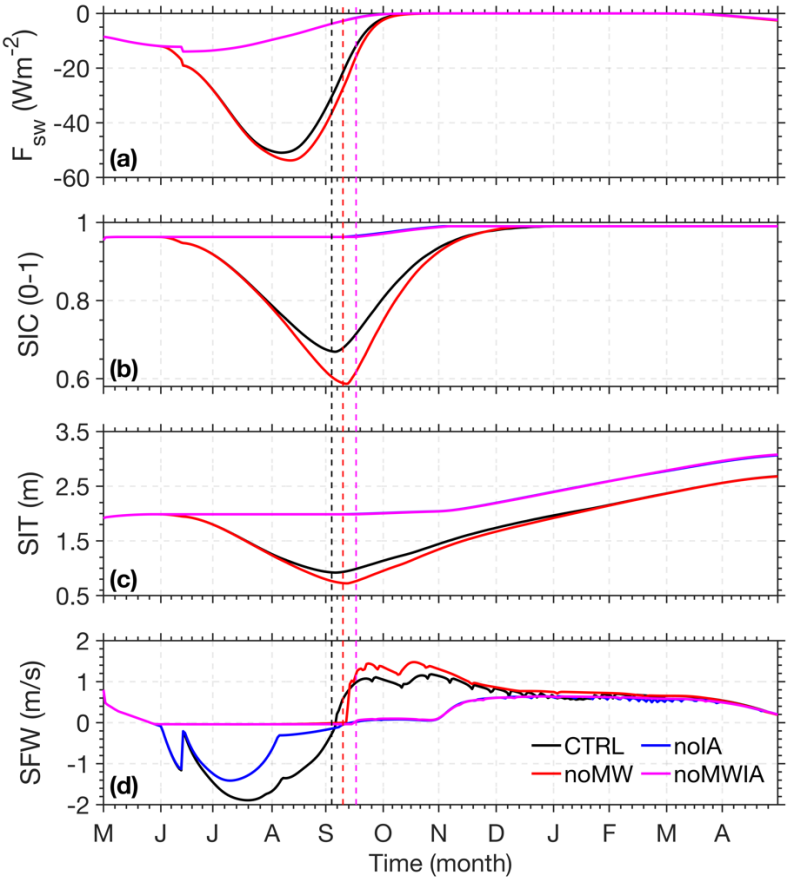

Figure 4. Modeled (a) net ocean shortwave heat flux, negative values represent heat entering the ocean. (b) ice concentration, (c) ice thickness and (d) net ocean surface freshwater flux at station BS5, negative values represent freshwater entering the ocean. The dashed lines perpendicular to the X-axis represent the first freezing day of each experiment (defined as the first day on which the ice thickness growth rate surpasses 0.1 cm/day).

3 Model results

The model results are not sensitive to small changes in initial profiles. Therefore, the experimental results for most of the initial profiles show qualitative consistency, except for the weakly stratified profiles, i.e., NS2-NS5, located in the Nansen basin. In order to show the general model behavior and the impact of ocean initial stratification, the detailed time developments of some model diagnostics are shown for two basic types of initial profiles, stations BS5 (strong stratification condition) and NS2 (weak stratification condition, as shown in Figure 2). For the other stations, we provide their modeled diagnostic averaged values in the melting and freezing season. In each experiment, the period before the first freezing day in September is defined as the melting season, while the period from the first freezing day to the end of the simulation is the freezing season. The first freezing

https://doi.org/10.5194/egusphere-2025-3030
Preprint. Discussion started: 7 August 2025

day is defined as the first day on which the ice thickness growth rate exceeds 0.1 cm/day. This section primarily presents and discusses the results from experiments with initial SIT of 2 m. Results for experiments with initial SIT of 1.5 m are provided in the SI (Figures S11-S13).

3.1 Sea Ice Response

3.1.1 Melting season

Figure 5a shows the thickness of sea ice melted during summer. When meltwater feedback is disabled (noMW), summer ice melting increases by 0.21 ± 0.01 m compared to the CTRL run, averaged value of experiments with initial SIT of 2 m. This implies that meltwater inhibits ice melting, thus establishing a negative feedback mechanism. Conversely, disabling ice-albedo feedback (noIA) reduces ice melting by 0.45 ± 0.02 m compared to the CTRL run, demonstrating that ice-albedo feedback is positive feedback that enhances summer ice melting.

When both feedbacks are suppressed (noMWIA), melting decreases by 0.39 ± 0.02 m relative to the CTRL run (Figure 5a). We can also notice that under conditions isolated from ice-albedo feedback (noIA and noMWIA), the presence of meltwater feedback (noIA) resulted in only 0.06 m less ice melting than its absence (noMWIA), demonstrating the negligible impact of meltwater feedback without ice-albedo feedback run (Figure 5a). This is not surprising, as less shortwave radiation flux leads to less ice melting. Furthermore, under conditions isolated from meltwater feedback (noMW and noMWIA in run Figure 5a), the presence of ice-albedo feedback (noMW) increased melting by 0.60 ± 0.02 m compared to its absence (noMWIA). These findings show that the ice-albedo feedback is the dominant process governing the Arctic sea ice-ocean system, which also significantly amplifies the efficacy of the meltwater-induced negative feedback.

3.1.2 Freezing season

During the freezing season, sea ice evolution is largely influenced by the stratification of the initial profile (Figure 5b). In the CTRL run of stations NS2-NS5, where stratification is weak, have less ice formation during winter (Figure 5b, CTRL). This is because, in areas with weak stratification, the brine rejection process during winter creates higher ocean-ice heat flux, which in turn inhibits ice formation, which is consistent with the results of Linders and Björk, (2013), who used a 1D model similar to this study to investigate the effect of initial ocean stratification on ice formation.

In the noMW run, ice formation in the strongly stratified regions is greater than in the CTRL run, whereas in the weakly stratified regions the ice formation is lower (noMW in Figure 5b). For example, at station BS5, with strong stratification, the removal of meltwater results in a 0.19 m increase in ice formation compared to the CTRL run, while at station NS2 with weak stratification, winter ice formation is reduced by 0.62 m. A notable phenomenon is that the ice melting event occurred in January at station NS2 (caused by the AWW mixing upward, more details discussed in Section 3.2), which is at least four

https://doi.org/10.5194/egusphere-2025-3030
Preprint. Discussion started: 7 August 2025

months earlier than the typical Arctic Ocean melting season, resulting in large ice-free areas in winter (FigureS14). This phenomenon is more pronounced in experiments with the initial SIT of 1.5 m (Figure S11b in SI). The noMWIA run also shows less ice formation compared to the noIA run (Figure 5b) in station NS2, NS4 and NS5, but no sea ice melting is observed during winter, further demonstrating the importance of meltwater in weakly stratified regions. In addition, the noIA and noMWIA runs show less ice formation compared to the CTRL and noMW runs (Figure 5b). This suggests that sea ice retreat during summer can promote ice formation in winter. Similarly, Keen et al. (2021), based on an analysis of CMIP6 models, found that basal growth increases in winter due to thinner sea ice during the 21st century. Lin et al. (2022) also observed this phenomenon from the ice mass balance buoys.

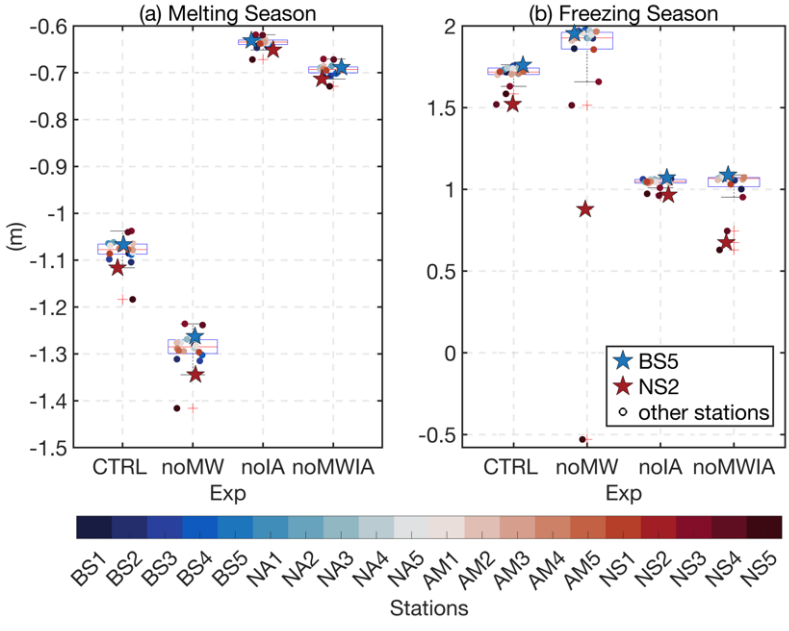

Figure 5. Box plots illustrating the (a) ice thickness changes during the melting season and (b) freezing season across different Stations in different types of experiments. Different stations are indicated by different colored dots. Each box plot shows the median, interquartile range, and potential outliers (points marked with red plus sign). All points are the results of experiments with initial SIT of 2 m.

3.2 Ocean Response

3.2.1 Melting season

It is apparent that removing meltwater feedback leads to a deeper, colder and saltier upper ocean during the melting season (Figure 6). Especially at stations with very weak initial stratification, the removal of meltwater leads to a much stronger deepening of the ML (Figure 6j and n). The most pronounced result is the disappearance of the NSTM following meltwater

https://doi.org/10.5194/egusphere-2025-3030
Preprint. Discussion started: 7 August 2025

removal (Figure 6b and d). At Station BS5, meltwater removal (noMW and noMWIA runs) increases the summer MLD to approximately 30 m (Figure 7a), which prevents the formation of the NSTM, because the heat absorbed by the ocean can mix sufficiently within the upper 30 m. Concurrently, the sea ice presence at surface maintains ML temperature at the freezing point, redirecting heat originally stored in the NSTM, isolated by meltwater, toward melting the ice. As demonstrated in Figures 8a and b, the noMW runs exhibit higher F_{oi} (ocean-ice heat flux) than CTRL, leading to an additional ice melting of 0.21 m. The F_{oi} has a significant seasonal cycle with maximum values reaching 40-60 W/m^2 in summer (Maykut and McPhee, 1995) and close to zero during winter in many instances (Krishfield and Perovich, 2005; McPhee et al., 2003; Zhong et al., 2022). The model results of the CTRL are in agreement with the observed values well (e.g., Fig. 8a and b, black lines).

Completely insulating the ice-albedo feedback leads to the ocean absorbing less heat (Figures 8c and d, blue and magenta lines) and results in the NSTM being cooler in the noIA run than in the CTRL run (Figure 7f). Naturally, the meltwater feedback effect is weaker because the heat insulated by meltwater is less in this case. F_{oi} in the noMWIA run increases by only ~ 2W/m^2 compared to the noIA run (Figures 8a and b, blue lines vs. magenta lines), leading to an additional ice melting of only 0.06 m, as discussed in section 3.1.

3.2.2 Freezing season

During the freezing season, in the noMW runs, the stations NS2-NS5 located in the Nansen basin, exhibit strong vertical mixing and much deeper MLD than other stations (Figure 7b). For example, at station NS2, the MLD deepens rapidly after December and reaches the core depth (~300 m) of the AWW by February, resulting in the upward mixing of AWW (Figures 6j and n). Concurrently, the F_{oi} significantly increases, reaching maximum values of 40 W/m² in the noMW run (Figure 8b), leading to nearly 22 cm of ice melting in the noMW run after February (Figure S14). Furthermore, the open water areas created by winter sea ice melting can release heat from the AWW into the atmosphere, with the maximum winter ocean-atmosphere heat fluxes (F_{oa}) reach about 100 W/m² in the noMW run (Figure 8f). In the experiment with initial SIT of 1.5 m, these phenomena are more pronounced, with sea ice melting approaching 2 m during winter (Figure S11 in SI), MLD exceeding 500 m (Figure S12 in SI) and F_{oa} greater than 200 W/m² at station NS2 (Figure S13 in SI). However, at stations in the Canadian and Amundsen basins, due to stronger initial stratification, while the ML obviously deepened after removing the meltwater, it still could not reach the warm water layer in the deep and the F_{oi} is nearly zero during winter (such as Figure 8a), which is insufficient to affect the surface sea ice.

In the noMWIA runs, the MLD during winter at station NS2 is only slightly deeper than in the noIA run (Figures 7b). Although the noMWIA run also removed meltwater, it does not exhibit the strong vertical mixing observed in the noMW run, indicating that the presence of sea ice effectively inhibits ocean vertical mixing and mitigates the effects of removing meltwater.

https://doi.org/10.5194/egusphere-2025-3030
Preprint. Discussion started: 7 August 2025

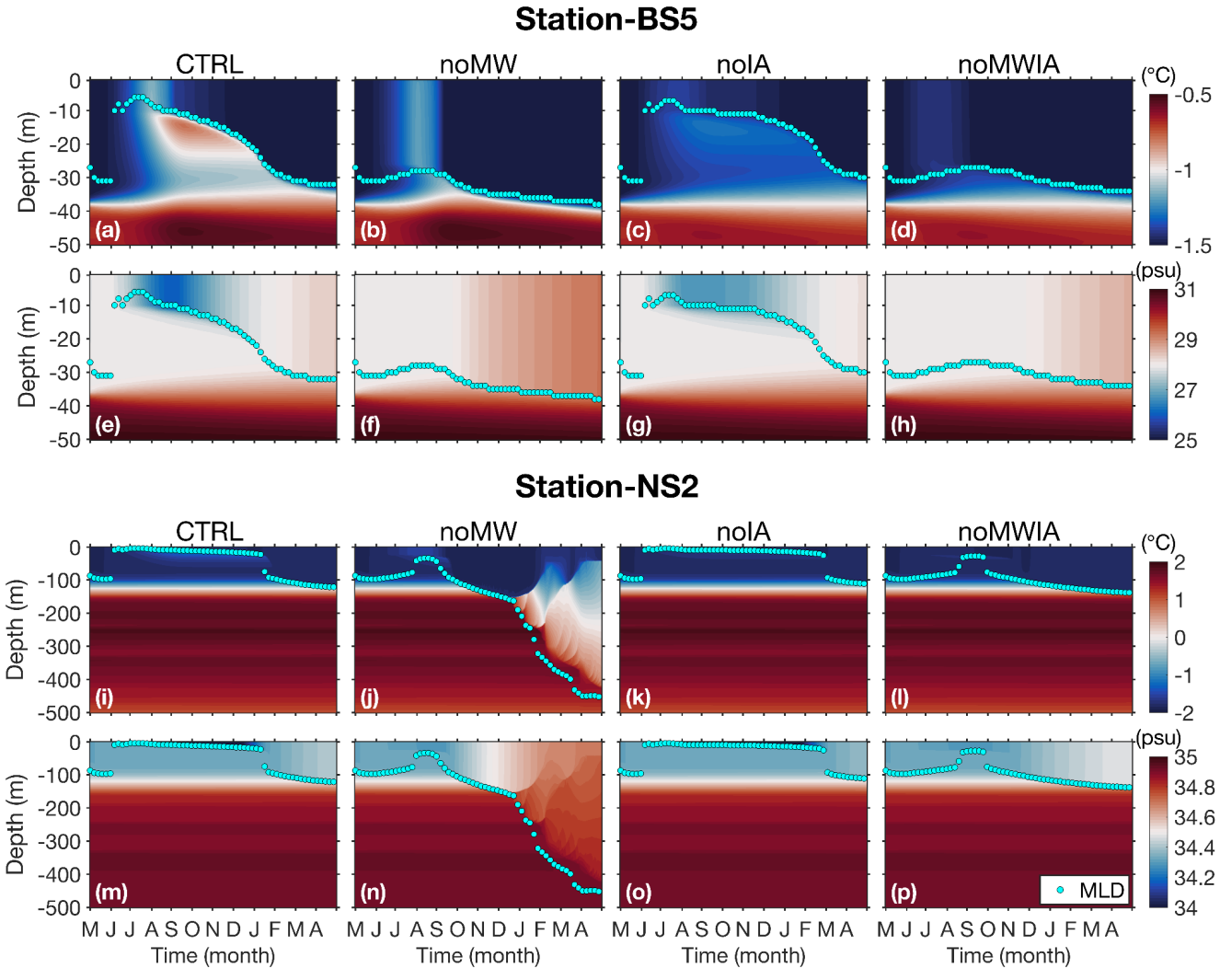

320

Figure 6. Time series of the vertical ocean (a)-(d) and (i)-(l): temperature and (e)-(h) and (m)-(p): salinity at station BS5 and NS2 for each experiment. The cyan dots represent the MLD in each experiment.

https://doi.org/10.5194/egusphere-2025-3030
Preprint. Discussion started: 7 August 2025

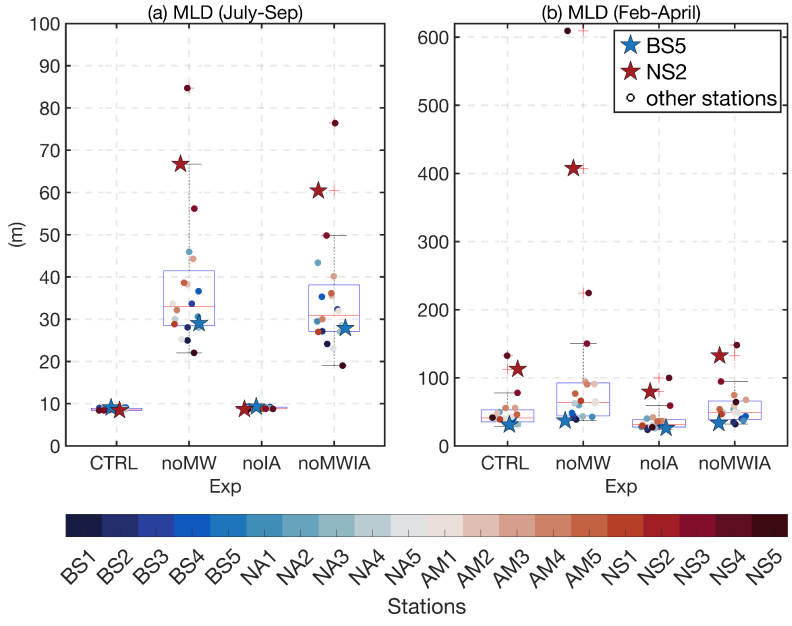

325 **Figure 7. Box plots illustrating the mean (a) MLD in summer and (b) winter across different Stations in different types of experiments. Different stations are indicated by different colored dots. Each box plot shows the median, interquartile range, and potential outliers (points marked with red plus sign). All points are the results of experiments with initial SIT of 2 m.**

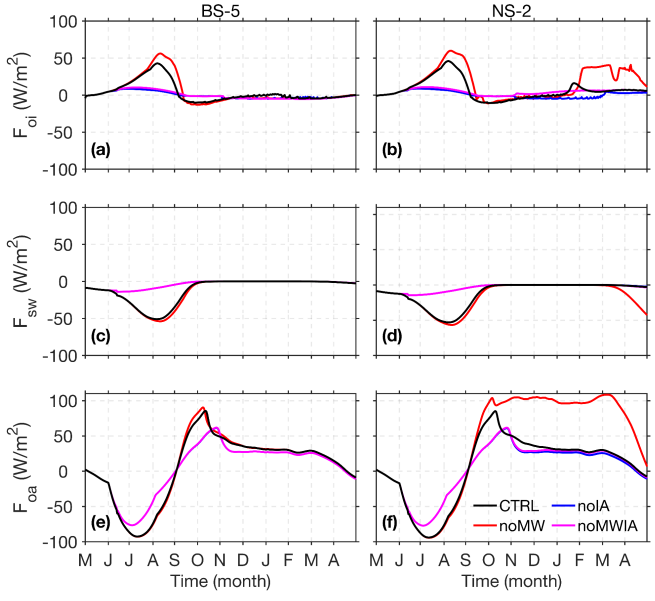

Figure 8. Heat flux time series at station BS5 (left column) and NS2 (right column). (a)-(b): F_{oi} (ocean-ice heat flux). (c)-(d): F_{sw}
330 **(solar shortwave flux into the ocean). (e)-(f) F_{oa} (ocean-atmosphere heat flux over the open ocean) for the experiments with initial SIT of 2 m. Positive (negative) values denote upward (downward) heat flux, corresponding to oceanic heat loss (gain).**

https://doi.org/10.5194/egusphere-2025-3030
Preprint. Discussion started: 7 August 2025

4 Quantifying Feedback Factors

This section quantifies meltwater and ice-albedo feedbacks using the feedback factor (γ) framework proposed by Goosse et al. (2018). Here, we focus on the meltwater and ice-albedo feedbacks to ice melting during the melting season, so, we selected the thickness of sea ice melted during the melting season as the reference variable. Based on the details of these decoupling experiments provided in Table1 and Figure 3, we can calculate the ice-albedo feedback factor (γ_{IA}) and meltwater feedback factor (γ_{MW}).

$$\gamma_{IA} = \frac{TR_{CTRL} - TR_{noIA}}{TR_{CTRL}} \quad (2)$$

$$\gamma_{MW} = \frac{TR_{CTRL} - TR_{noMW}}{TR_{CTRL}} \quad (3)$$

here, TR_{CTRL}, TR_{noIA} and TR_{noMW} are the thickness of sea ice melted during the melting season in the CTRL (full system including all the feedbacks), noIA (ice-albedo feedback not operating) and noMW (meltwater feedback not operating) runs, respectively (as shown in Figure 5a).

Additionally, our experimental design provides a framework to quantify the net effects of meltwater and ice-albedo feedbacks by preventing each from the influence of one another. The net ice-albedo feedback factor (γ_{nIA}) and the net meltwater feedback factor (γ_{nMW}):

$$\gamma_{nIA} = \frac{TR_{noMW} - TR_{noMWIA}}{TR_{noMW}} \quad (4)$$

$$\gamma_{nMW} = \frac{TR_{noIA} - TR_{noMWIA}}{TR_{noIA}} \quad (5)$$

where TR_{noMWIA} is the thickness of sea ice melted during the melting season in the noMWIA run (both meltwater and ice-albedo feedbacks not operating).

Figure 9 shows the feedback factors for all stations. We can notice that although Figure 5a shows differences in summer sea ice melt thickness among the stations, the calculated feedback factors remain very close. The results indicate that the positive ice-albedo feedback ($\gamma_{IA} = +0.41$) is approximately twice as strong as the negative meltwater feedback ($\gamma_{MW} = -0.19$). When ice-albedo feedback is fully eliminated, the negative meltwater feedback strength decreases to $\gamma_{nMW} = -0.09$ (Figure 9). The albedo feedback factor only increased from +0.41 to +0.46 after preventing the meltwater feedback. In fact, when the feedback factor is expressed as a percentage, it represents the percentage increase or decrease in sea ice melting relative to the reference experiment (i.e., the denominator in Eq. (2)-(5)). Based on this, a schematic diagram is presented herein, as presented in Figure 10 showing the values of each feedback factor and the percentage change in sea ice melting thickness between experiments.

https://doi.org/10.5194/egusphere-2025-3030
Preprint. Discussion started: 7 August 2025

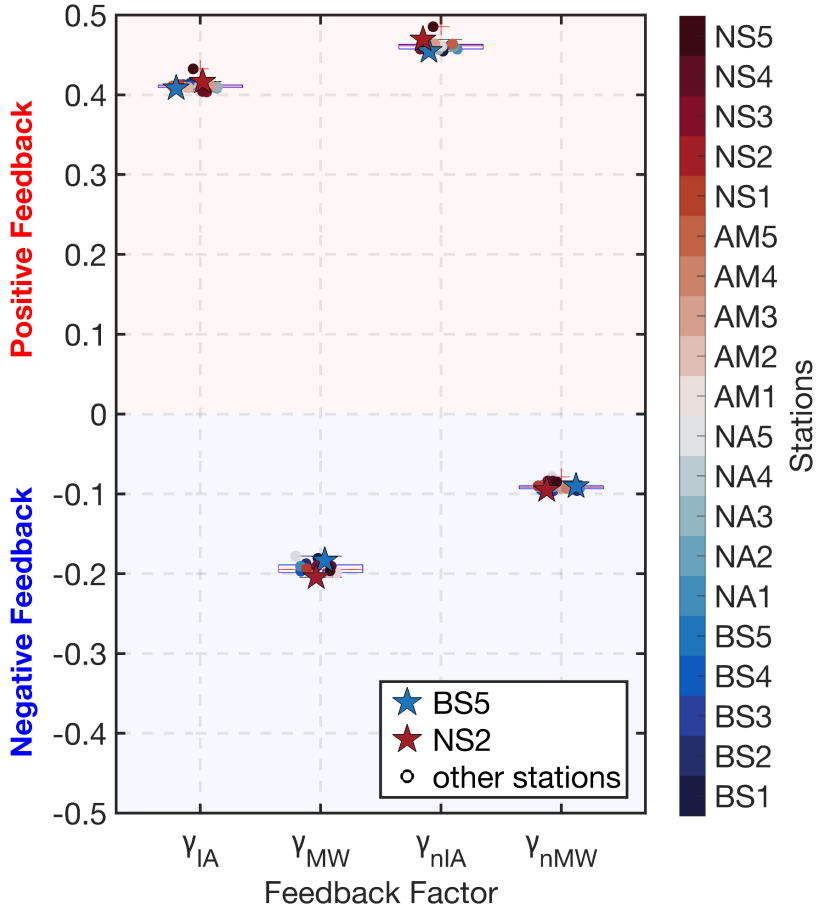

Figure 9. Box plots illustrating the four feedback factors across different Stations. If the γ is a positive (negative) value, it represents positive (negative) feedback. All points are the results of experiments with initial SIT of 2 m. The blue star and red star represent stations BS5 and NS2, respectively. Ice-albedo feedback Factor: γ_{IA}; Meltwater feedback Factor: γ_{MW}; Net meltwater feedback factor: γ_{nIA}; Net ice-albedo feedback factor: γ_{nMW}.

https://doi.org/10.5194/egusphere-2025-3030
Preprint. Discussion started: 7 August 2025

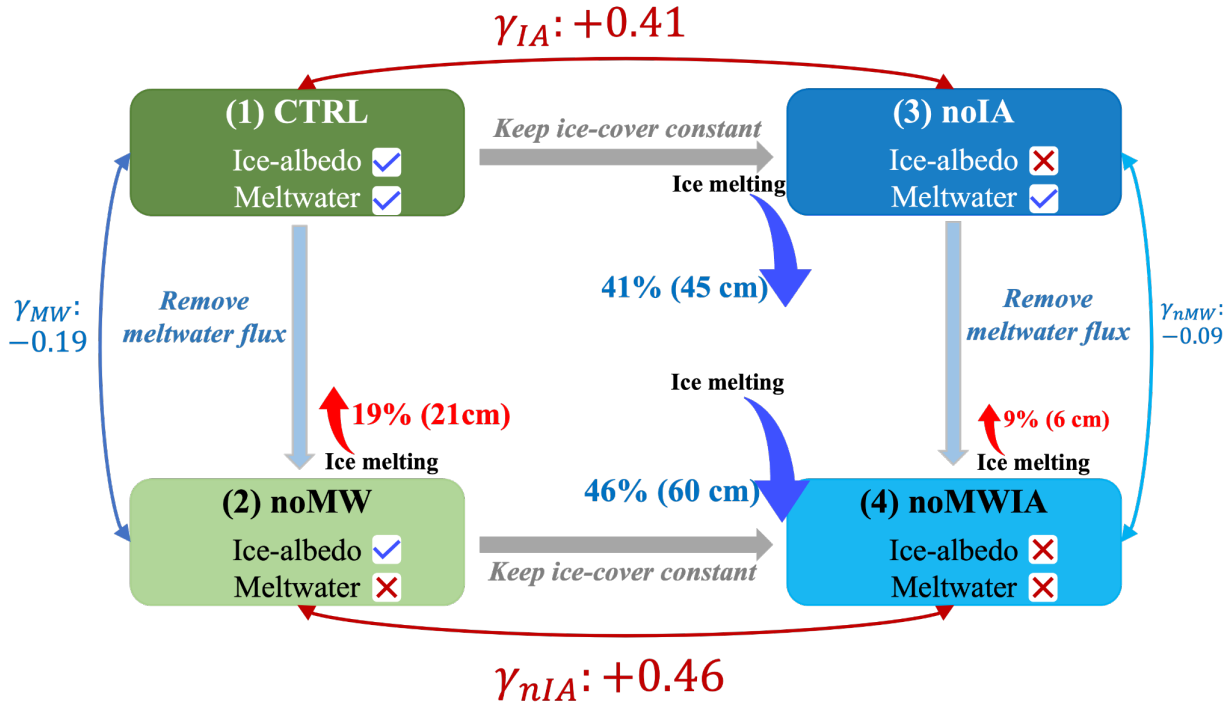

Figure 10. Schematic of the relationships between four experimental setups for studying ice-albedo and meltwater feedbacks. The blue checkmark indicates that the feedback is existent, and the red cross indicates that the feedback is eliminated. The blue or red double-headed arrow between two experiments signifies the comparison of these results and the corresponding feedback factors obtained. The red upward arrow indicates the increase in ice melting, while the red downward arrow indicates the decrease in ice melting. Left Side: With albedo feedback present, removing meltwater feedback results in a 19% increase in ice melting; Right Side: Without albedo feedback, removing meltwater feedback leads to a 9% increase in ice melting; Top Side: With meltwater feedback present, removing albedo feedback causes a 41% decrease in ice melting; Bottom Side: Without meltwater feedback, removing albedo feedback results in a 46% decrease in ice melting.

5 Discussion

Using a simple 1D coupled sea ice-ocean model, this study demonstrated that meltwater feedback plays a crucial role in ice melting, with its feedback factor reaching up to half of the ice-albedo feedback factor. The strength of meltwater feedback depends strongly on ice-albedo feedback, when the ice-albedo feedback is eliminated, the meltwater feedback factor decreases from -0.19 to -0.09 (the negative sign corresponding to negative feedback). The 1D model excludes advection flux processes, thus not accounting for lateral heat and freshwater fluxes. In regions of the Arctic Ocean near the Fram Strait, the heat flux from the Atlantic water inflow significantly impacts the ice-ocean system (Polyakov et al., 2017; Timmermans et al., 2018). However, this study focuses solely on short-term, seasonal-scale vertical changes, and the presence or absence of bottom temperature and salinity recovery during the one-year simulation period does not significantly affect the model results.

https://doi.org/10.5194/egusphere-2025-3030
Preprint. Discussion started: 7 August 2025

Although the study is carried out in an idealized framework, its design, initial conditions, and forcing closely follow the actual mean state of the Arctic Ocean, and the seasonal variations in the vertical structure, ice-ocean heat flux of the Arctic Ocean are accurately reproduced in the CTRL run. Thus, the results of this experiment are reliable.

A relevant summer meltwater feedback process in model development is the melt pond, which collects the surface meltwater, and can cover up to 50 to 60% of the sea ice surface (Eicken et al., 2004; Fetterer and Untersteiner, 1998; Diamond et al., 2021). The presence of melt pools not only increases melting by absorbing more radiation at the ice surface, but also by concentrating more meltwater on the ice surface rather than releasing it into the ocean. This is a process similar to the noMW run, where less meltwater entering the ocean accelerates sea ice melting. Therefore, improving the performance of melt pond formation, as well as meltwater release processes in coupled ice-sea models is very important for accurately modeling the Arctic Ocean.

The impacts of meltwater on the subsequent freezing season exhibit significant regional differences. In strongly stratified regions, the removal of meltwater prevents NSTM formation and leads to larger open water areas at the onset of winter, thereby promoting more ice formation. Steele et al., (2011) reported similar results, showing that the heat content of the autumn NSTM is sufficient to melt 1 m of sea ice during the subsequent winter, and is more likely to occur under conditions of strong surface wind fields (Jackson et al., 2012; Alvarez, 2023). Our experimental findings are consistent with those of Davis et al., (2016), who examined the competing effects of freshwater input and vertical mixing in an 1D model, and the results indicate that enhanced vertical mixing plays a more significant role in sea ice melting in the Eurasian Basin. In weakly stratified areas of our study, such as stations NS2, NS4 and NS5 located in the western Nansen Basin, AWW can mix upward and melt sea ice in winter if there is no 'protective layer' formed by meltwater. In particular, at station NS5, where the AWW layer lies close to the surface due to its proximity to the Barents Sea (Figure 2k), exhibited more sea ice melting (Figure 5b) and a deeper MLD (Figure 7b) during winter in the noMW run, despite having stronger stratification than NS2 and NS4 (Figure 2l). A model-based study by Linders and Björk, (2013) also observed the phenomenon of constant or decreasing ice thickness during winter and large ocean-ice heat flux in the Nansen Basin close to the Fram Strait, because Atlantic water is more easily mixed upward due to the influence of the West Spitsbergen Current. In addition, we used climatological data from World Ocean Atlas 2023 (WOA2023, Reagan et al., 2024) as the ocean initial conditions to conduct simulations in each basin (Figure S15 in SI), and the results persistently show that the removal of meltwater leads to upward mixing of AWW and ice melting in winter at western Nansen Basin (Figure S16 in SI), with 0.4 m and 0.06 m of winter ice melting in experiments with initial SIT of 1.5 m and 2 m, respectively (Figure S17i and Figure S18i in SI). These pervious studies and our results based on the climatological conditions demonstrate that the intense vertical mixing and ice melting during the winter in the Nansen Basin is not a coincidental event caused by the initial profile selection.

Some observations and model results show that Eurasian Basin has become less stratified (Lique et al., 2018; Muilwijk et al., 2023; Polyakov et al., 2018, 2020), due to the freshwater redistribution (Morison et al., 2012; Solomon et al., 2021; Q. Wang et al., 2019) and Arctic Atlantification (Barton et al., 2018; Polyakov et al., 2017; Tesi et al., 2021). As Atlantification of the Arctic Ocean accelerates, the area of weak stratification in the Eurasian basin will continue to expand, and meltwater

https://doi.org/10.5194/egusphere-2025-3030
Preprint. Discussion started: 7 August 2025

will play an increasingly important role in regulating air-ice-ocean interactions. When sea ice retreats to a point where not enough meltwater is produced during the summer to maintain the stratification, and there is also not enough sea ice on the surface to impede atmosphere-ocean interactions, then the heat from the AWW may mix sufficiently upward and be released into the atmosphere, which could have serious implications for the Arctic ice-ocean system (Turner, 2010; Richards et al., 2022).

This study primarily focuses on quantifying meltwater and ice-albedo feedbacks during summer, as well as the effects of meltwater on the ice-ocean system in the subsequent winter. However, the winter sea-ice formation process also contains many feedbacks as well, which require more in-depth studies. For example, the ice production-entrainment feedback, where brine rejection during sea ice formation brings heat from the deep to the surface, melts part of the ice initially formed and inhibits further ice production (Goosse et al., 2018; Martinson, 1990; Martinson and Iannuzzi, 1998), and the ice growth-thickness feedback, where thin sea ice grows more rapidly than thick sea ice due to its higher heat conduction (Bitz and Roe, 2004), a phenomenon that has been observed recently in the Arctic ocean (Lin et al., 2022). Indeed, these two winter feedbacks are already reflected in our experiments. For example, the CTRL runs show less sea ice production during winter in the weakly stratified station (NS2-NS5) compared with other stations (Figure 5b), which is primarily driven by the ice production-entrainment feedback. More sea ice growth in the CTRL run than in the noIA run (Figure 5b), which corresponds to the ice growth-thickness feedback. Additionally, the increased atmospheric energy input due to sea ice changes is crucial for the ice-ocean system, as thinner sea ice results in stronger ocean surface shear (Martin et al., 2016; Polyakov et al., 2020). In our study, for instance, in the noMWIA run at station NS2, the absence of meltwater did not lead to the intense mixing observed in the noMW run during winter, highlighting the importance of sea ice in limiting vertical mixing in weakly stratified regions. The wind input feedback induced by the sea ice reduction process also needs to be further understood and quantified. While here we focus on inter-seasonal changes during a full melting-freezing season, understanding the changes in stratification over inter-annual timescales is an appealing extension of our modelling framework, for instance, examining the contribution of rapidly declining sea ice and warmer atmospheric forcing conditions to future Atlantification of the Arctic Ocean, but it is beyond the scope of the present work.

6 Conclusions

Using a well-validated 1D coupled sea ice-ocean model and a series of decoupling experiments in conjunction with a simple and consistent method for quantifying feedback factors, this study quantifies the independent roles of meltwater and ice-albedo feedbacks in Arctic sea ice melting and examines their impacts on the subsequent freezing seasons. To the best of our knowledge, this is the first study to quantify the above feedback effects, both individually and in combination, in the ice-ocean system. Based on the model results, the key findings are:

https://doi.org/10.5194/egusphere-2025-3030
Preprint. Discussion started: 7 August 2025

1. During the melting season, the negative feedback induced by meltwater reaches approximately half the strength of the positive ice-albedo feedback ($\gamma_{MW} = -0.19$ vs. $\gamma_{IA} = +0.41$), demonstrating the significant role of meltwater in regulating ice-ocean interactions.
2. Meltwater reduces total summer ice melting by approximately 19%, and when ice-albedo feedback is eliminated (i.e., ice cover is fixed), this number decreases to 9%, indicating that ice-albedo processes dominate the meltwater feedback.
3. The ice-albedo feedback increases sea ice melting by 41%, and when the meltwater negative feedback is removed, this number only rises to 46%, further demonstrating the dominant role of ice-albedo feedback in the ice-ocean system.
4. Meltwater affects the subsequent freezing season differently across regions: in strongly stratified areas, it delays winter ice melting by slowing surface cooling, whereas in the weakly stratified Nansen Basin, it promotes ice freezing by isolating AWW from ice. These effects are amplified under thinner initial ice conditions, suggesting growing importance of meltwater as Arctic sea ice declines and transitions toward seasonal coverage.

Appendix A

The thermodynamic ice model is based on the 3-layer model by Winton (2000) and the energy-conserving LANL CICE model (Bitz and Lipscomb, 1999). The sea ice model configuration includes two equally thick ice layers: the upper layer has variable specific heat resulting from brine pockets, and the lower layer has a fixed heat capacity. A zero-heat capacity snow layer lies above the ice. Net heat fluxes at the ice top (F_{top}, W/m2) and bottom surfaces (F_{bot}, W/m2) are used to calculate the change in ice and snow layer thickness:

$$F_{top} = F_s - \frac{4k_i k_s (T_2 - T_f)}{k_s h_s + 4k_i h_i}(T_s - T_1) \quad \text{(A1)}$$

$$F_{bot} = \frac{k_i (T_2 - T_f)}{h_i} - F_{oi} \quad \text{(A2)}$$

in which, k_i and k_s are the constant thermal conductivity of ice and snow respectively; F_s is net energy flux from the atmosphere to the ice, which can cause melt at the ice top or basal growth at the ice bottom by heat conduction through ice; T_s is the skin surface temperature; T_1 and T_2 are the temperatures of the upper and lower layers of ice, respectively. T_f is the freezing point. h_i and h_s are the sea ice and snow thickness. Δt is the model timestep (600 s). F_{oi} is the ocean-ice heat flux that is used for basal melt at the ice bottom face ($T_{sst} > T_f$, in which T_{sst} is the sea surface temperature), or is the freezing potential for new ice formation over open waters ($T_{sst} < T_f$), i.e., when ocean temperature fall below the freezing temperature, F_{oi} is equivalent to the heat energy required to keep the ocean temperature from falling below freezing (Maykut and McPhee, 1995).

$$F_{oi} = c_{sw}\rho_{sw}\gamma(T_{sst} - T_f)u^*, \quad T_{sst} > T_f \quad \text{(A3)}$$

$$F_{oi} = \frac{c_f \rho_f (T_f - T_{sst})\Delta z}{\Delta t}, \quad T_{sst} < T_f \quad \text{(A4)}$$

https://doi.org/10.5194/egusphere-2025-3030
Preprint. Discussion started: 7 August 2025

in which, c_{sw} and ρ_{sw} are the heat capacity and density of the seawater, respectively. γ (=0.006) is the heat transfer coefficient. c_f and ρ_f are the specific heat and density of liquid freshwater, respectively. $u^* = \sqrt{|\tau_w|/\rho_{sw}|}$ is the frictional velocity between ice and water, with minimum value of $u^* = 0.005$, in which τ_w is the ice-ocean stress.

If $F_{top} > 0$, the model melts snow from the surface, if all the snow is melted and there is energy left, the model melts the ice, and the sea ice growth and melt rates (Δh_i, m/s) at the atmosphere-ice (top) and ocean-ice (bottom) interfaces at each time step can be described by:

$$\Delta h_i = \frac{-F_{top/bot}}{q\rho_i}\Delta t \quad \text{(A5)}$$

in which q and ρ_i are the enthalpy and density of ice, respectively.

The albedo parameterization of the thermodynamic ice model is:

$$\alpha = f_s\alpha_s + (1 - f_s)(\alpha_{imin} + (\alpha_{imax} - \alpha_{imin})(1 - e^{-h_i/h_{ia}})) \quad \text{(A6)}$$

where f_s is 1 if there is snow and 0 if not, $\alpha_{imin}(= 0.2)$ and $\alpha_{imax}(= 0.66)$ are ice albedos for thin and thick bare ice respectively, and h_{ia} $(= 0.8)$ is a scale height for ice albedo. The α_s is the snow albedo, depending on whether $T_s < 0$ or not:

$$\alpha_s = \alpha_{coldSnow} + (\alpha_{warmSnow} - \alpha_{coldSnow}) \cdot max(0, min(1 - T_s\ /h_{sa})) \quad \text{(A7)}$$

where $\alpha_{coldSnow}$ $(= 0.85)$ and $\alpha_{warmSnow}$ $(= 0.7)$ are snow albedos for cold and warm snow respectively, and h_{sa} $(= 0.3)$ is a scale height for snow albedo. For open-ocean area, the albedo is 0.08.

Data availability

The Ice-Tethered Profiler data were collected and made available by the Ice-Tethered Profiler Program based at the Woods Hole Oceanographic Institution (Krishfield et al., 2008; Toole et al., 2011) and are available at https://doi.org/10.7289/v5mw2f7x (Toole et al., 2016). NCEP/DOE Reanalysis II data provided by the NOAA PSL, Boulder, Colorado, USA (https://psl.noaa.gov). The World Ocean Database 2018 and World Ocean Atlas 2023 are available through the National Centers for Environmental Information (NCEI) archives (https://www.ncei.noaa.gov/products/). The monthly ice thickness and concentration are permanently deposited to NSIDC, https://nsidc.org/data/.The 1D model configuration, parameters and forcing fields used in this study are stored at https://github.com/HaohZhang/1D-model.

Author contributions

HH conducted the experiments and model validation, analyzed the data, and drafted the initial version of the manuscript. AS and CY designed the experiments. HH and XB Conducted the 1D model construction and code modification based on the MITgcm. HH, AS, XB and CY all participated in the review and editing of this paper.

https://doi.org/10.5194/egusphere-2025-3030
Preprint. Discussion started: 7 August 2025

Competing interests

Neither of the authors has any competing interests.

Acknowledgments

This work was funded by the National Natural Science Foundation of China (Grant No. 42276254). Haohao Zhang was also supported by the scholarship from China Scholarship Council (Grant No. 202306710085).

References

Aagaard, K., Coachman, L. K., and Carmack, E. (1981). On the halocline of the Arctic Ocean. Deep Sea Research Part A. Oceanographic Research Papers, 28(6), 529–545. https://doi.org/10.1016/0198-0149(81)90115-1

Alkire, M. B., Morison, J., Schweiger, A., Zhang, J., Steele, M., Peralta-Ferriz, C., and Dickinson, S. (2017). A Meteoric Water Budget for the Arctic Ocean. Journal of Geophysical Research: Oceans, 122(12), 10020–10041. https://doi.org/10.1002/2017JC012807

Alvarez, A.: A model for the Arctic mixed layer circulation under a summertime lead: implications for the near-surface temperature maximum formation, The Cryosphere, 17, 3343–3361, https://doi.org/10.5194/tc-17-3343-2023, 2023.

Armitage, T. W. K., Manucharyan, G. E., Petty, A. A., Kwok, R., and Thompson, A. F. (2020). Enhanced eddy activity in the Beaufort Gyre in response to sea ice loss. Nature Communications, 11(1), 761. https://doi.org/10.1038/s41467-020-14449-z

Barton, B. I., Lenn, Y.-D., and Lique, C. (2018). Observed Atlantification of the Barents Sea Causes the Polar Front to Limit the Expansion of Winter Sea Ice. Journal of Physical Oceanography, https://doi.org/10.1175/JPO-D-18-0003.1

Bitz, C. M., and Lipscomb, W. H. (1999). An energy-conserving thermodynamic model of sea ice. Journal of Geophysical Research: Oceans, 104(C7), 15669–15677. https://doi.org/10.1029/1999JC900100

Bitz, C. M., and G. H. Roe, 2004: A Mechanism for the High Rate of Sea Ice Thinning in the Arctic Ocean. Journal of Climate, 17, 3623–3632, https://doi.org/10.1175/1520-0442(2004)017<3623:AMFTHR>2.0.CO;2.

Carmack, E. C., Yamamoto-Kawai, M., Haine, T. W. N., Bacon, S., Bluhm, B. A., Lique, C., et al. (2016). Freshwater and its role in the Arctic Marine System: Sources, disposition, storage, export, and physical and biogeochemical consequences in the Arctic and global oceans. Journal of Geophysical Research: Biogeosciences, 121(3), 675–717. https://doi.org/10.1002/2015JG003140

Davis, P. E. D., Lique, C., Johnson, H. L., and Guthrie, J. D. (2016). Competing Effects of Elevated Vertical Mixing and Increased Freshwater Input on the Stratification and Sea Ice Cover in a Changing Arctic Ocean. Journal of Physical Oceanography, 46(5), 1531–1553. https://doi.org/10.1175/JPO-D-15-0174.1

https://doi.org/10.5194/egusphere-2025-3030
Preprint. Discussion started: 7 August 2025

Diamond, R., Sime, L. C., Schroeder, D., and Guarino, M.-V.: The contribution of melt ponds to enhanced Arctic sea-ice melt during the Last Interglacial, The Cryosphere, 15, 5099–5114, https://doi.org/10.5194/tc-15-5099-2021, 2021.

Eicken, H., Grenfell, T. C., Perovich, D. K., Richter-Menge, J. A., and Frey, K. (2004). Hydraulic controls of summer Arctic pack ice albedo. Journal of Geophysical Research: Oceans, 109(C8). https://doi.org/10.1029/2003JC001989

Fer, I. (2009). Weak Vertical Diffusion Allows Maintenance of Cold Halocline in the Central Arctic. Atmospheric and Oceanic Science Letters, 2(3), 148–152. https://doi.org/10.1080/16742834.2009.11446789

Fetterer, F., and Untersteiner, N. (1998). Observations of melt ponds on Arctic sea ice. Journal of Geophysical Research: Oceans, 103(C11), 24821–24835. https://doi.org/10.1029/98JC02034

Fine, E. C., McClean, J. L., Ivanova, D. P., Craig, A. P., Wallcraft, A. J., Chassignet, E. P., and Hunke, E. C. (2023). Arctic ice-ocean interactions in an 8-to-2 kilometer resolution global model. Ocean Modelling, 184, 102228. https://doi.org/10.1016/j.ocemod.2023.102228

Forryan, A., Bacon, S., Tsubouchi, T., Torres-Valdés, S., and Naveira Garabato, A. C.: Arctic freshwater fluxes: sources, tracer budgets and inconsistencies, The Cryosphere, 13, 2111–2131, https://doi.org/10.5194/tc-13-2111-2019, 2019.

Goosse, H., Kay, J. E., Armour, K. C., Bodas-Salcedo, A., Chepfer, H., Docquier, D., et al. (2018). Quantifying climate feedbacks in polar regions. Nature Communications, 9(1), 1919. https://doi.org/10.1038/s41467-018-04173-0

Haine, T. W. N., Curry, B., Gerdes, R., Hansen, E., Karcher, M., Lee, C., et al. (2015). Arctic freshwater export: Status, mechanisms, and prospects. Global and Planetary Change, 125, 13–35. https://doi.org/10.1016/j.gloplacha.2014.11.013

Himmich, K., Vancoppenolle, M., Stammerjohn, S., Bocquet, M., Madec, G., Sallée, J.-B., and Fleury, S. (2024). Thermodynamics Drive Post-2016 Changes in the Antarctic Sea Ice Seasonal Cycle. Journal of Geophysical Research: Oceans, 129(8), e2024JC021112. https://doi.org/10.1029/2024JC021112

Holland, M. M., Bitz, C. M., and Tremblay, B. (2006). Future abrupt reductions in the summer Arctic Sea ice. Geophysical Research Letters, 33(23). https://doi.org/10.1029/2006GL028024

Hordoir, R., Skagseth, Ø., Ingvaldsen, R. B., Sandø, A. B., Löptien, U., Dietze, H., et al. (2022). Changes in Arctic Stratification and Mixed Layer Depth Cycle: A Modeling Analysis. Journal of Geophysical Research: Oceans, 127(1), e2021JC017270. https://doi.org/10.1029/2021JC017270

Hunke, E.C and W.H. Lipscomb, circa 2001: CICE: the Los Alamos Sea Ice Model Documentation and Software User's Manual. LACC-98-16v.2.

Hudson, S. R., Granskog, M. A., Sundfjord, A., Randelhoff, A., Renner, A. H. H., and Divine, D. V. (2013). Energy budget of first-year Arctic sea ice in advanced stages of melt. Geophysical Research Letters, 40(11), 2679–2683. https://doi.org/10.1002/grl.50517

Jackett, D. R., and T. J. Mcdougall, 1995: Minimal Adjustment of Hydrographic Profiles to Achieve Static Stability. J. Atmos. Oceanic Technol., 12, 381–389, https://doi.org/10.1175/1520-0426(1995)012<0381:MAOHPT>2.0.CO;2.

https://doi.org/10.5194/egusphere-2025-3030
Preprint. Discussion started: 7 August 2025

Jackson, J. M., Carmack, E. C., McLaughlin, F. A., Allen, S. E., and Ingram, R. G. (2010). Identification, characterization, and change of the near-surface temperature maximum in the Canada Basin, 1993–2008. Journal of Geophysical Research: Oceans, 115(C5). https://doi.org/10.1029/2009JC005265

Jackson, J. M., Williams, W. J., and Carmack, E. C.: Winter sea-ice melt in the Canada Basin, Arctic Ocean: Winter Sea – ice melt Canada basin, Geophys. Res. Lett., 39, L03603, https://doi.org/10.1029/2011GL050219, 2012.

Jenkins, M., and Dai, A. (2021). The Impact of Sea-Ice Loss on Arctic Climate Feedbacks and Their Role for Arctic Amplification. Geophysical Research Letters, 48(15), e2021GL094599. https://doi.org/10.1029/2021GL094599

Kacimi, S., and Kwok, R. (2022). Arctic Snow Depth, Ice Thickness, and Volume From ICESat-2 and CryoSat-2: 2018–2021. Geophysical Research Letters, 49(5), e2021GL097448. https://doi.org/10.1029/2021GL097448

Kanamitsu, M., Ebisuzaki, W., Woollen, J., Yang, S.-K., Hnilo, J. J., Fiorino, M., and Potter, G. L. (2002). NCEP–DOE AMIP-II Reanalysis (R-2). https://doi.org/10.1175/BAMS-83-11-1631

Keen, A., Blockley, E., Bailey, D. A., Boldingh Debernard, J., Bushuk, M., Delhaye, S., Docquier, D., Feltham, D., Massonnet, F., O'Farrell, S., Ponsoni, L., Rodriguez, J. M., Schroeder, D., Swart, N., Toyoda, T., Tsujino, H., Vancoppenolle, M., and Wyser, K.: An inter-comparison of the mass budget of the Arctic sea ice in CMIP6 models, The Cryosphere, 15, 951–982, https://doi.org/10.5194/tc-15-951-2021, 2021.

Krishfield, R. A., and Perovich, D. K. (2005). Spatial and temporal variability of oceanic heat flux to the Arctic ice pack. Journal of Geophysical Research, 110, C07021. https://doi.org/10.1029/2004JC002293

Krishfield, R., Toole, J., Proshutinsky, A., and Timmermans, M.-L. (2008). Automated Ice-Tethered Profilers for Seawater Observations under Pack Ice in All Seasons. https://doi.org/10.1175/2008JTECHO587.1

Krishfield, R. A., Proshutinsky, A., Tateyama, K., Williams, W. J., Carmack, E. C., McLaughlin, F. A., and Timmermans, M.-L. (2014). Deterioration of perennial sea ice in the Beaufort Gyre from 2003 to 2012 and its impact on the oceanic freshwater cycle. Journal of Geophysical Research: Oceans, 119(2), 1271–1305. https://doi.org/10.1002/2013JC008999

Kwok, R. (2018). Arctic sea ice thickness, volume, and multiyear ice coverage: losses and coupled variability (1958–2018). Environmental Research Letters, 13(10), 105005. https://doi.org/10.1088/1748-9326/aae3ec

Kwok, R., Kacimi, S., Webster, M. a., Kurtz, N. t., and Petty, A. a. (2020). Arctic Snow Depth and Sea Ice Thickness From ICESat-2 and CryoSat-2 Freeboards: A First Examination. Journal of Geophysical Research: Oceans, 125(3), e2019JC016008. https://doi.org/10.1029/2019JC016008

Landy, J. C., Dawson, G. J., Tsamados, M., Bushuk, M., Stroeve, J. C., Howell, S. E. L., et al. (2022). A year-round satellite sea-ice thickness record from CryoSat-2. Nature, 609(7927), 517–522. https://doi.org/10.1038/s41586-022-05058-5

Landrum, L. L. and Holland, M. M.: Influences of changing sea ice and snow thicknesses on simulated Arctic winter heat fluxes, The Cryosphere, 16, 1483–1495, https://doi.org/10.5194/tc-16-1483-2022, 2022.

https://doi.org/10.5194/egusphere-2025-3030
Preprint. Discussion started: 7 August 2025

Large, W. G., McWilliams, J. C., and Doney, S. C. (1994). Oceanic vertical mixing: A review and a model with a nonlocal boundary layer parameterization. Reviews of Geophysics, 32(4), 363–403. https://doi.org/10.1029/94RG01872

Liang, X., and Losch, M. (2018). On the Effects of Increased Vertical Mixing on the Arctic Ocean and Sea Ice. Journal of Geophysical Research: Oceans, 123(12), 9266–9282. https://doi.org/10.1029/2018JC014303

Lin, L., Lei, R., Hoppmann, M., Perovich, D. K., and He, H.: Changes in the annual sea ice freeze–thaw cycle in the Arctic Ocean from 2001 to 2018, The Cryosphere, 16, 4779–4796, https://doi.org/10.5194/tc-16-4779-2022, 2022.

Linders, J., and Björk, G. (2013). The melt-freeze cycle of the Arctic Ocean ice cover and its dependence on ocean stratification. Journal of Geophysical Research: Oceans, 118(11), 5963–5976. https://doi.org/10.1002/jgrc.20409

Lique, C., Johnson, H. L., and Plancherel, Y. (2018). Emergence of deep convection in the Arctic Ocean under a warming climate. Climate Dynamics, 50(9), 3833–3847. https://doi.org/10.1007/s00382-017-3849-9

Losch, M., Menemenlis, D., Campin, J.-M., Heimbach, P., & Hill, C. (2010). On the formulation of sea-ice models. Part 1: Effects of different solver implementations and parameterizations. *Ocean Modelling*, *33*(1), 129–144. https://doi.org/10.1016/j.ocemod.2009.12.008

Marshall, J., Hill, C., Perelman, L., and Adcroft, A. (1997). Hydrostatic, quasi-hydrostatic, and nonhydrostatic ocean modeling. Journal of Geophysical Research: Oceans, 102(C3), 5733–5752. https://doi.org/10.1029/96JC02776

Martin, T., Tsamados, M., Schroeder, D., and Feltham, D. L. (2016). The impact of variable sea ice roughness on changes in Arctic Ocean surface stress: A model study. Journal of Geophysical Research: Oceans, 121(3), 1931–1952. https://doi.org/10.1002/2015JC011186

Martinson, D. G. (1990). Evolution of the southern ocean winter mixed layer and sea ice: Open ocean deepwater formation and ventilation. Journal of Geophysical Research: Oceans, 95(C7), 11641–11654. https://doi.org/10.1029/JC095iC07p11641

Martinson, D. G., and Iannuzzi, R. A. (1998). Antarctic Ocean-Ice Interaction: Implications from Ocean Bulk Property Distributions in the Weddell Gyre. In Antarctic Sea Ice: Physical Processes, Interactions and Variability (pp. 243–271). American Geophysical Union (AGU). https://doi.org/10.1029/AR074p0243

Maykut, G. A., and McPhee, M. G. (1995). Solar heating of the Arctic mixed layer. Journal of Geophysical Research: Oceans, 100(C12), 24691–24703. https://doi.org/10.1029/95JC02554

McPhee, M. G., Kikuchi, T., Morison, J. H., and Stanton, T. P. (2003). Ocean-to-ice heat flux at the North Pole environmental observatory. Geophysical Research Letters, 30(24), 2274. https://doi.org/10.1029/2003GL018580

Mioduszewski, J. R., Vavrus, S., Wang, M., Holland, M., and Landrum, L.: Past and future interannual variability in Arctic sea ice in coupled climate models, The Cryosphere, 13, 113–124, https://doi.org/10.5194/tc-13-113-2019, 2019.

Mishonov A.V., T. P. Boyer, O. K. Baranova, C. N. Bouchard, S. Cross, H. E. Garcia, R. A. Locarnini, C. R. Paver, J. R. Reagan, Z. Wang, D. Seidov, A. I. Grodsky, J. G. Beauchamp, (2024): World Ocean Database 2023. C. Bouchard, Technical Ed., NOAA Atlas NESDIS 97, 206 pp., doi.org/10.25923/z885-h264,

https://doi.org/10.5194/egusphere-2025-3030
Preprint. Discussion started: 7 August 2025

Moon, T. A. and Druckenmiller, M. L. and Thoman, R. L. "Arctic Report Card 2021: Executive Summary" (2021), https://doi.org/10.25923/5s0f-5163

Morison, J., and Smith, J. D. (1981). Seasonal variations in the upper Arctic Ocean as observed at T-3. Geophysical Research Letters, 8(7), 753–756. https://doi.org/10.1029/GL008i007p00753

Morison, J., Kwok, R., Peralta-Ferriz, C., Alkire, M., Rigor, I., Andersen, R., and Steele, M. (2012). Changing Arctic Ocean freshwater pathways. Nature, 481(7379), 66–70. https://doi.org/10.1038/nature10705

Muilwijk, M., A. Nummelin, C. Heuzé, I. V. Polyakov, H. Zanowski, and L. H. Smedsrud, 2023: Divergence in Climate Model Projections of Future Arctic Atlantification. Journal of Climate, 36, 1727–1748, https://doi.org/10.1175/JCLI-D-22-0349.1.

Nguyen, A. T., Menemenlis, D., and Kwok, R. (2011). Arctic ice-ocean simulation with optimized model parameters: Approach and assessment. Journal of Geophysical Research, 116(C4), C04025. https://doi.org/10.1029/2010JC006573

Nummelin, A., Li, C., and Smedsrud, L. H. (2015). Response of Arctic Ocean stratification to changing river runoff in a column model. Journal of Geophysical Research: Oceans, 120(4), 2655–2675. https://doi.org/10.1002/2014JC010571

Nummelin, A., Ilicak, M., Li, C., and Smedsrud, L. H. (2016). Consequences of future increased Arctic runoff on Arctic Ocean stratification, circulation, and sea ice cover. Journal of Geophysical Research: Oceans, 121(1), 617–637. https://doi.org/10.1002/2015JC011156

Osadchiev, A. A., Izhitskiy, A. S., Zavialov, P. O., Kremenetskiy, V. V., Polukhin, A. A., Pelevin, V. V., and Toktamysova, Z. M. (2017). Structure of the buoyant plume formed by Ob and Yenisei river discharge in the southern part of the Kara Sea during summer and autumn. Journal of Geophysical Research: Oceans, 122(7), 5916–5935. https://doi.org/10.1002/2016JC012603

Osadchiev, A. A., Frey, D. I., Shchuka, S. A., Tilinina, N. D., Morozov, E. G., and Zavialov, P. O. (2021). Structure of the Freshened Surface Layer in the Kara Sea During Ice-Free Periods. Journal of Geophysical Research: Oceans, 126(1), e2020JC016486. https://doi.org/10.1029/2020JC016486

Peralta-Ferriz, C., and Woodgate, R. A. (2015). Seasonal and interannual variability of pan-Arctic surface mixed layer properties from 1979 to 2012 from hydrographic data, and the dominance of stratification for multiyear mixed layer depth shoaling. Progress in Oceanography, 134, 19–53. https://doi.org/10.1016/j.pocean.2014.12.005

Perovich, D., Smith, M., Light, B., and Webster, M.: Meltwater sources and sinks for multiyear Arctic sea ice in summer, The Cryosphere, 15, 4517–4525, https://doi.org/10.5194/tc-15-4517-2021, 2021.

Polyakov, I. V., Bhatt, U. S., Walsh, J. E., Abrahamsen, E. P., Pnyushkov, A. V., and Wassmann, P. F. (2013). Recent oceanic changes in the Arctic in the context of long-term observations. Ecological Applications, 23(8), 1745–1764. https://doi.org/10.1890/11-0902.1

https://doi.org/10.5194/egusphere-2025-3030
Preprint. Discussion started: 7 August 2025

Polyakov, I. V., Pnyushkov, A. V., Alkire, M. B., Ashik, I. M., Baumann, T. M., Carmack, E. C., et al. (2017). Greater role for Atlantic inflows on sea-ice loss in the Eurasian Basin of the Arctic Ocean. Science, 356(6335), 285–291. https://doi.org/10.1126/science.aai8204

Polyakov, I. V., Pnyushkov, A. V., and Carmack, E. C. (2018). Stability of the arctic halocline: a new indicator of arctic climate change. Environmental Research Letters, 13(12), 125008. https://doi.org/10.1088/1748-9326/aaec1e

Polyakov, I. V., Rippeth, T. P., Fer, I., Baumann, T. M., Carmack, E. C., Ivanov, V. V., et al. (2020). Intensification of Near-Surface Currents and Shear in the Eastern Arctic Ocean. Geophysical Research Letters, 47(16), e2020GL089469. https://doi.org/10.1029/2020GL089469

Polyakov, I. V., and Coauthors, 2020: Weakening of Cold Halocline Layer Exposes Sea Ice to Oceanic Heat in the Eastern Arctic Ocean. Journal of Climate, 33, 8107–8123, https://doi.org/10.1175/JCLI-D-19-0976.1.

Rainville, L., and Winsor, P. (2008). Mixing across the Arctic Ocean: Microstructure observations during the Beringia 2005 Expedition. Geophysical Research Letters, 35(8). https://doi.org/10.1029/2008GL033532

Reagan, James R.; Boyer, Tim P.; García, Hernán E.; Locarnini, Ricardo A.; Baranova, Olga K.; Bouchard, Courtney; Cross, Scott L.; Mishonov, Alexey V.; Paver, Christopher R.; Seidov, Dan; Wang, Zhankun; Dukhovskoy, Dmitry. (2024). World Ocean Atlas 2023. NOAA National Centers for Environmental Information. Dataset: NCEI Accession 0270533.

Richards, A. E., Johnson, H. L., and Lique, C. (2022). Spatial and temporal variability of Atlantic Water in the Arctic from 40 years of observations. Journal of Geophysical Research: Oceans, 127, e2021JC018358. https://doi.org/10.1029/2021JC018358.

Rudels, B., Anderson, L. G., and Jones, E. P. (1996). Formation and evolution of the surface mixed layer and halocline of the Arctic Ocean. Journal of Geophysical Research: Oceans, 101(C4), 8807–8821. https://doi.org/10.1029/96JC00143

Rudels, Bert, Jones, E. P., Schauer, U., and Eriksson, P. (2004). Atlantic sources of the Arctic Ocean surface and halocline waters. Polar Research, 23(2), 181–208. https://doi.org/10.3402/polar.v23i2.6278

Serreze, M. C., and Meier, W. N. (2019). The Arctic's sea ice cover: trends, variability, predictability, and comparisons to the Antarctic. Annals of the New York Academy of Sciences, 1436(1), 36–53. https://doi.org/10.1111/nyas.13856

Serreze, M. C., Barrett, A. P., Slater, A. G., Woodgate, R. A., Aagaard, K., Lammers, R. B., et al. (2006). The large-scale freshwater cycle of the Arctic. Journal of Geophysical Research: Oceans, 111(C11). https://doi.org/10.1029/2005JC003424

Shaw, W. J., and Stanton, T. P. (2014). Vertical diffusivity of the Western Arctic Ocean halocline. Journal of Geophysical Research: Oceans, 119(8), 5017–5038. https://doi.org/10.1002/2013JC009598

Shimada, K., Kamoshida, T., Itoh, M., Nishino, S., Carmack, E., McLaughlin, F., et al. (2006). Pacific Ocean inflow: Influence on catastrophic reduction of sea ice cover in the Arctic Ocean. Geophysical Research Letters, 33(8), 2005GL025624. https://doi.org/10.1029/2005GL025624

https://doi.org/10.5194/egusphere-2025-3030
Preprint. Discussion started: 7 August 2025

Smith, M., Stammerjohn, S., Persson, O., Rainville, L., Liu, G., Perrie, W., et al. (2018). Episodic Reversal of Autumn Ice Advance Caused by Release of Ocean Heat in the Beaufort Sea. Journal of Geophysical Research: Oceans, 123(5), 3164–3185. https://doi.org/10.1002/2018JC013764

Solomon, A., Heuzé, C., Rabe, B., Bacon, S., Bertino, L., Heimbach, P., et al. (2021). Freshwater in the Arctic Ocean 2010–2019. Ocean Science, 17(4), 1081–1102. https://doi.org/10.5194/os-17-1081-2021

Steele, M., and Boyd, T. (1998). Retreat of the cold halocline layer in the Arctic Ocean. Journal of Geophysical Research: Oceans, 103(C5), 10419–10435. https://doi.org/10.1029/98JC00580

Steele, M., Ermold, W., and Zhang, J. (2011). Modeling the formation and fate of the near-surface temperature maximum in the Canadian Basin of the Arctic Ocean. Journal of Geophysical Research: Oceans, 116(C11). https://doi.org/10.1029/2010JC006803

Sumata, H., de Steur, L., Divine, D.V. et al. Regime shift in Arctic Ocean sea ice thickness. Nature 615, 443–449 (2023). https://doi.org/10.1038/s41586-022-05686-x

Tesi, T., Muschitiello, F., Mollenhauer, G., Miserocchi, S., Langone, L., Ceccarelli, C., et al. (2021). Rapid Atlantification along the Fram Strait at the beginning of the 20th century. Science Advances, 7(48), eabj2946. https://doi.org/10.1126/sciadv.abj2946

Thackeray, C. W., and Hall, A. (2019). An emergent constraint on future Arctic sea-ice albedo feedback. Nature Climate Change, 9(12), 972–978. https://doi.org/10.1038/s41558-019-0619-1

Timmermans, M.-L., Marshall, J., Proshutinsky, A., and Scott, J. (2017). Seasonally derived components of the Canada Basin halocline. Geophysical Research Letters, 44(10), 5008–5015. https://doi.org/10.1002/2017GL073042

Timmermans, M.-L., Toole, J., and Krishfield, R. (2018). Warming of the interior Arctic Ocean linked to sea ice losses at the basin margins. Science Advances, 4(8), eaat6773. https://doi.org/10.1126/sciadv.aat6773

Toole, J. M., Timmermans, M.-L., Perovich, D. K., Krishfield, R. A., Proshutinsky, A., and Richter-Menge, J. A. (2010). Influences of the ocean surface mixed layer and thermohaline stratification on Arctic Sea ice in the central Canada Basin. Journal of Geophysical Research: Oceans, 115(C10). https://doi.org/10.1029/2009JC005660

Toole, J. M., Krishfield, R. A., Timmermans, M.-L., and Proshutinsky, A. (2011). The ice-tethered profiler: Argo of the Arctic. Oceanography, 24(3), 126–135. https://doi.org/10.5670/oceanog.2011.64

Toole, J. M., Krishfield, R., O'Brien, J. K., Houk, A. E., Cole, S. T., and Program, W. H. (2016). Ice-tethered profiler observations: Vertical profiles of temperature, salinity, oxygen, and ocean velocity from an ice-tethered profiler buoy system [Dataset]. NOAA National Centers for Environmental Information. https://doi.org/10.7289/v5mw2f7x

Turner, J. S. (2010). The melting of ice in the Arctic Ocean: The influence of double-diffusive transport of heat from below. Journal of Physical Oceanography, 40(1), 249–256. https://doi.org/10.1175/2009JPO4279.1.

Uhlíková, T., Vihma, T., Karpechko, A. Y., and Uotila, P.: Effects of Arctic sea-ice concentration on surface radiative fluxes in four atmospheric reanalyses, The Cryosphere, 19, 1031–1046, https://doi.org/10.5194/tc-19-1031-2025, 2025.

https://doi.org/10.5194/egusphere-2025-3030
Preprint. Discussion started: 7 August 2025

Wang, Q., Wekerle, C., Danilov, S., Sidorenko, D., Koldunov, N., Sein, D., et al. (2019). Recent Sea Ice Decline Did Not Significantly Increase the Total Liquid Freshwater Content of the Arctic Ocean. Journal of Climate, https://doi.org/10.1175/JCLI-D-18-0237.1

Wang, Q., Danilov, S., Sidorenko, D., and Wang, X. (2021). Circulation Pathways and Exports of Arctic River Runoff Influenced by Atmospheric Circulation Regimes. Frontiers in Marine Science, 8, 707593. https://doi.org/10.3389/fmars.2021.707593

Wang, Y., Feng, Z., Lin, P., Song, H., Zhang, J., Wu, H., et al. (2024). Enhanced wind mixing and deepened mixed layer in the Pacific Arctic shelf seas with low summer sea ice. Nature Communications, 15(1), 10389. https://doi.org/10.1038/s41467-024-54733-w

Winton, M. (2000). A Reformulated Three-Layer Sea Ice Model. Retrieved from https://journals.ametsoc.org/view/journals/atot/17/4/1520-0426_2000_017_0525_artlsi_2_0_co_2.xml

Winton, M. (2006). Does the Arctic sea ice have a tipping point? Geophysical Research Letters, 33(23). https://doi.org/10.1029/2006GL028017

Zhong, W., Cole, S. T., Zhang, J., Lei, R., and Steele, M. (2022). Increasing winter ocean-to-ice heat flux in the Beaufort Gyre region, Arctic Ocean over 2006–2018. Geophysical Research Letters, 49, e2021GL096216. https://doi.org/10.1029/2021GL096216

Zhang, H., Bai, X., and Wang, K. (2023). Response of the Arctic sea ice–ocean system to meltwater perturbations based on a one-dimensional model study. Ocean Science, 19(6), 1649–1668. https://doi.org/10.5194/os-19-1649-2023